# High-Coercivity Samarium-Iron-Nitrogen from Nitriding Melt-Spun Ribbons

*F.E. Pinkerton and C.D. Fuerst*

**Melt spinning has proven to be an excellent technique for magnetic hardening of a variety of permanent magnet materials, especially Nd-Fe-B. Recently, a new permanent magnet material has been discovered by nitriding the compound $Sm_2Fe_{17}$ to obtain $Sm_2Fe_{17}N_x$. The authors have obtained magnetically hard Sm-Fe-N ribbons with a room-temperature intrinsic coercivity $H_{ci}$ = 22 kOe (1.8 MA/m) by nitriding melt-spun Sm-Fe precursor ribbons. Best results were obtained by grinding the ribbons to a <25 μm powder, then heat treating the powder in vacuum for 1 h at 700 °C prior to nitriding in $N_2$ gas at 450 to 480 °C. X-ray diffraction shows that the primary phase is $TbCu_7$-type $Sm_2Fe_{17}N_x$, a disordered hexagonal modification of the rhombohedral $Sm_2Fe_{17}$ phase.**

**Keywords**

magnetic materials, melt-spun ribbons, nitriding, permanent magnet, samarium alloys, samarium-iron oxide

## 1. Introduction

INSPIRED by the discovery of Nd-Fe-B magnets,[1,2] the past decade has witnessed an unprecedented growth in the research and development of novel permanent magnet materials. The combination of the new ternary phase $Nd_2Fe_{14}B$[3] with magnetic hardening by melt spinning[4]—Magnequench™—has opened an innovative avenue to explore the science and technology of these new magnet materials. From its early success with Nd-Fe-B, rapid quenching has been extended to obtain high intrinsic coercivities, $H_{ci}$, in a variety of candidate materials, such as $ThMn_{12}$-type compounds (e.g., $SmFe_{10}V_2$[5] and $SmFe_{11}Ti$[6]) and Sm-rich $Sm_{20}Fe_{70}Ti_{10}$.[7]

Recently, Coey and co-workers have discovered a new class of candidate permanent magnet materials based on nitriding the known binary phase $Sm_2Fe_{17}$.[8,9] The nitrided compound retains the rhombohedral $Th_2Zn_{17}$ structure of the binary phase, with the nitrogen atoms absorbed interstitially. Recent extended X-ray absorption fine-structure (EXAFS) analysis of the $Sm_2Fe_{17}N_x$ compound[10] has shown that the nitrogen atoms occupy the interstitial 9*e* sites in the $Th_2Zn_{17}$-type structure, with $x \sim 3$, corroborating neutron diffraction results on the isostructural nitrides $Y_2Fe_{17}N_x$ and $Nd_2Fe_{17}N_x$.[11] The resulting lattice expansion has a profound impact on the intrinsic magnetic properties; the Curie temperature, for example, increases by about 350 °C. $Sm_2Fe_{17}$ is the most important compound for permanent magnets, because nitriding of the Sm representative also generates a large uniaxial magnetocrystalline anisotropy.[8,9] Similar results are obtained for $Sm_2Fe_{17}C_x$ carbides[12] and more recently for nitrides in the $ThMn_{12}$-type compounds, such as $NdFe_{11}Ti$[13] and $NdFe_{10}Mo_2$.[14]

**F.E. Pinkerton** and **C.D. Fuerst**, Physics Department, General Motors NAO Research and Development Center, Warren, Michigan.

In this article, the focus is on magnetic hardening of $Sm_2Fe_{17}N_x$-based materials using melt spinning. As recently reported, coercivities as large as 22 kOe (1.8 MA/m) are obtained by nitriding precursor materials based on melt-spun $Sm_2Fe_{17}$.[15] The current results are very similar to those previously reported by Katter et al.[16]

## 2. Melt Spinning and Nitriding of Sm-Fe Precursor Ribbons

The strategy adopted for obtaining high-coercivity Sm-Fe-N relies on melt spinning Sm-Fe precursor ribbons followed by gas phase nitriding. The melt spinning technique, illustrated schematically in Fig. 1, is the same used to rapidly quench Nd-Fe-B magnet materials.[4] First, a starting $Sm_{15}Fe_{85}$ ingot was made by induction melting stoichiometric quantities of elemental Sm and Fe in a BN crucible. Pieces of the ingot were then placed in a quartz crucible with a 0.65-mm orifice in the bottom. The alloy was induction melted, and the molten metal was ejected through the orifice by a 24-kPa overpressure of Ar

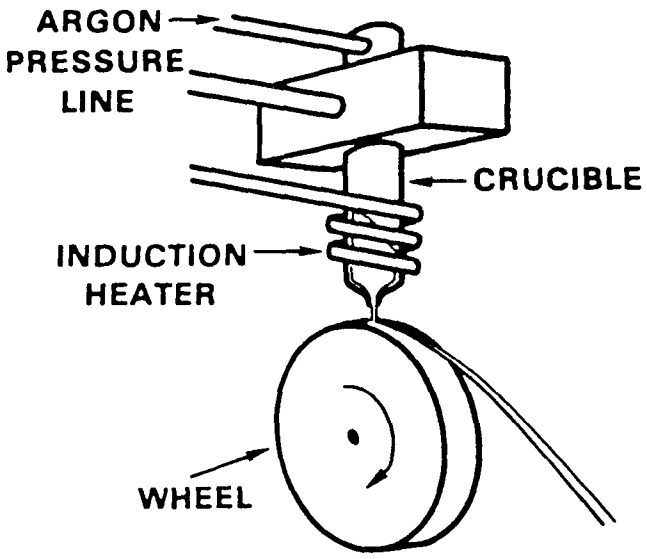


**Fig. 1** Schematic of the melt spinning process.

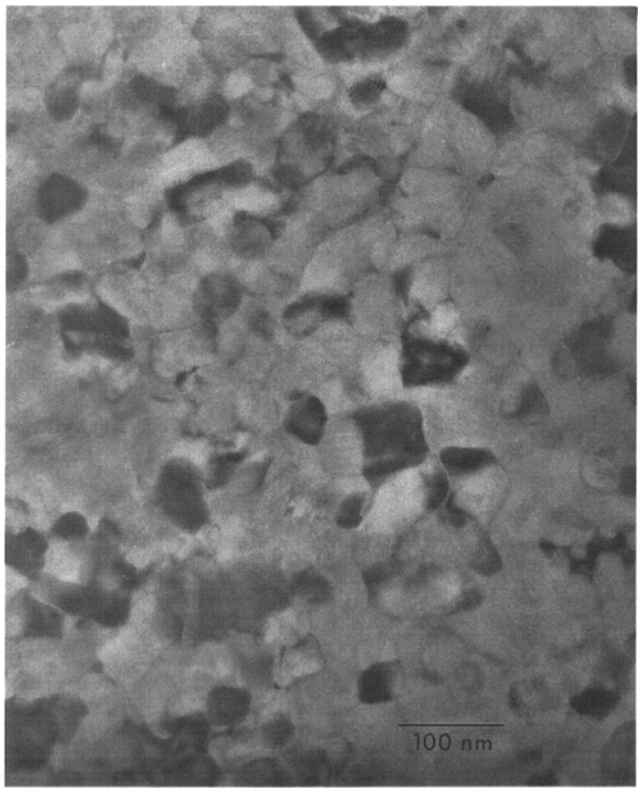


**Fig. 2** Transmission electron micrograph of melt-spun Sm-Fe ribbons.

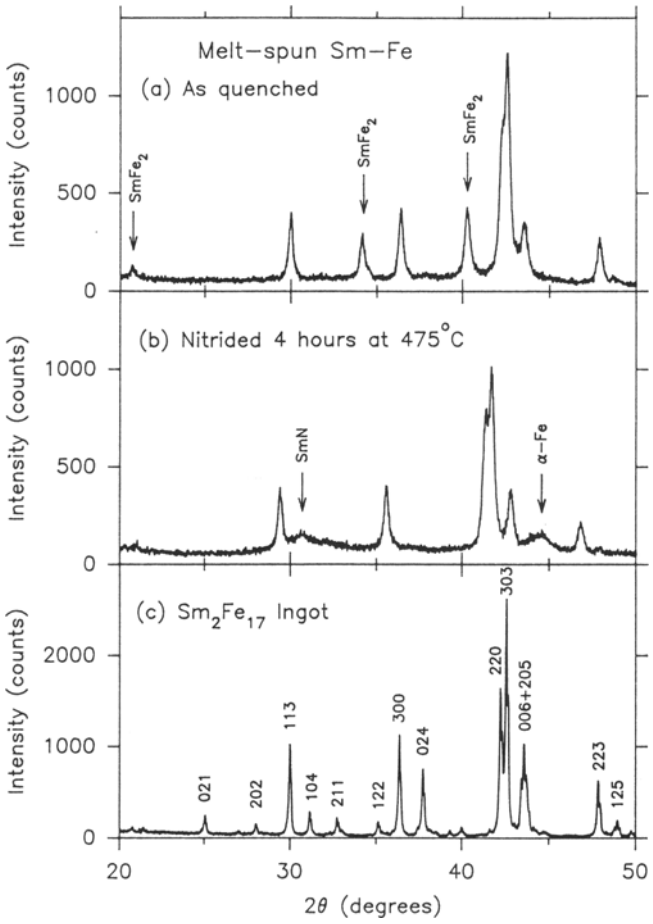


**Fig. 3** X-ray diffraction patterns for (a) Sm-Fe ribbons quenched at a wheel velocity of 35 m/s, (b) nitrided for 4 h at 475 °C in $N_2$ gas, and (c) $Sm_2Fe_{17}$ ingot.

gas. Upon striking the circumference of the Cr-plated copper quench wheel, rotating with a surface velocity of 35 m/s, the molten alloy solidified into a ribbon approximately 1 mm wide and 30 μm thick. Processing was done in a chamber containing a protective atmosphere of Ar gas. Inductively coupled plasma atomic emission spectrometry (ICP/AES) analysis showed the final ribbon composition to be $Sm_{14.5}Fe_{85.5}$, the balance of Sm having been lost by vaporization during processing.

The microstructure of the as-spun Sm-Fe ribbons, shown by the transmission electron micrograph in Fig. 2, is very similar to that observed in melt-spun Nd-Fe-B ribbons.[17] It is predominantly a single-phase microstructure consisting of very fine grains, less than about 40 nm in diameter. Contrast between the grains indicates that there is a thin intergranular layer between each grain, again similar to the microstructure observed in Nd-Fe-B ribbons, comprising perhaps 2 to 3% of the sample volume. The chemistry obtained by energy dispersive X-ray spectrometry (EDX), taken over a large number of grains, is very close to the $Sm_2Fe_{17}$ stoichiometry. Some grains contain a background contrast characteristic of a twinned structure; in these grains, EDX shows a slightly Fe-deficient composition, with an overall stoichiometry of about $Sm_2Fe_{15}$. The shapes of the grains are quite variable, which is one indication that the microstructure is far from equilibrium.

The similitude of the Sm-Fe ribbon microstructure to that of Nd-Fe-B ribbons, wherein magnetic hardness arises from the very fine $Nd_2Fe_{14}B$ grain size (20 to 80 nm in a simple, nonequilibrium microstructure) gives promise that this precursor can be magnetically hardened by nitriding to generate the favorable intrinsic magnetic properties of $Sm_2Fe_{17}N_x$. Gas phase nitriding was done on mechanically ground ribbon powder having a particle size smaller than 45 μm (–325 mesh). The ribbons were heat treated inside a quartz tube with a regulated 140-kPa atmosphere of pure $N_2$ gas. Heat treatments were carried out at temperatures of 450 to 480 °C for times ranging from 1 to 65 h. The heating rate was set by inserting the gas-filled tube into the furnace, and after heat treatment, the tube was air cooled.

## 3. Structure and Properties of Sm-Fe-N

### 3.1 *X-Ray Diffraction*

The X-ray diffraction pattern for melt-spun Sm-Fe before nitriding is shown in Fig. 3(a). The sample is composed primarily of a $Sm_2Fe_{17}$-like phase, with $SmFe_2$ occurring as a second phase. The major diffraction peaks correspond very well with the major peaks of the $Sm_2Fe_{17}$ phase. However, comparison with the X-ray diffraction pattern of $Sm_2Fe_{17}$ ingot (Fig. 3c) shows that a number of minor peaks in the $Sm_2Fe_{17}$ pattern are

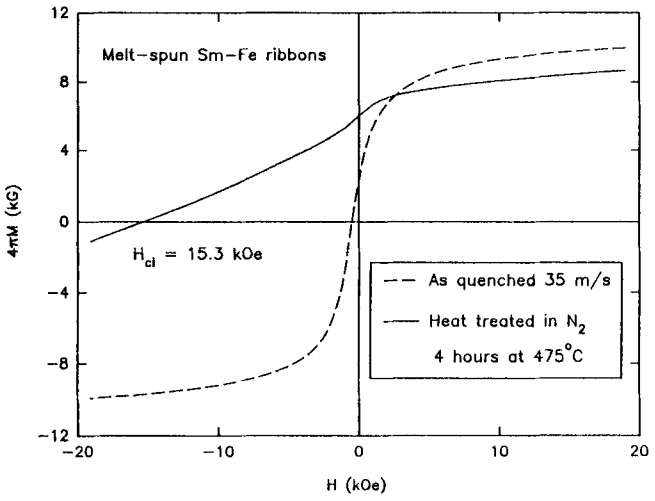


**Fig. 4** Demagnetization curves for Sm-Fe ribbons prior to nitriding (dashed curve) and after nitriding for 4 h at 475 °C (solid curve).

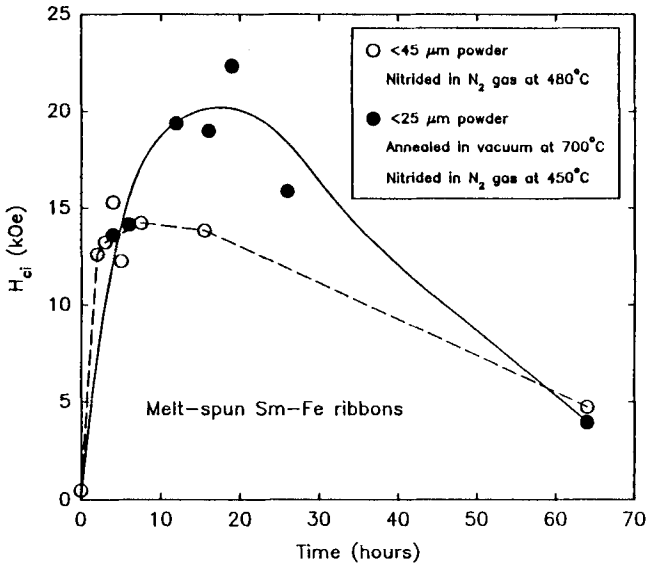


**Fig. 5** $H_{ci}$ as a function of nitriding time. Open circles: <45 μm powder with no prenitriding heat treatment. Closed circles: <25 μm powder, 1 h at 700 °C prior to nitriding.

missing in the ribbons, most notably the 024 peak. This simplified pattern is characteristic of a disordered variant of $Th_2Zn_{17}$, the hexagonal $TbCu_7$ structure.[18] The rhombohedral $Th_2Zn_{17}$ structure is formed from the hexagonal $CaCu_5$-type structure characteristic of compounds such as $SmCo_5$ by an ordered replacement of one third of the rare earth atoms by pairs of transition metal atoms (the dumbbell sites). The $TbCu_7$ structure arises when the replacement is random rather than ordered. The $Th_2Zn_{17}$ structure can therefore be considered to be an ordered superstructure of the $TbCu_7$ structure.[18]

The dominance of the disordered $TbCu_7$ structure is a clear indication of the nonequilibrium nature of the melt-spun ribbons. Another is the presence of the $SmFe_2$ phase. In the equilibrium phase diagram, a $Sm_{14.5}Fe_{85.5}$ alloy would form a mixture of $Sm_2Fe_{17}$ and $SmFe_3$ phases. The absence of the $SmFe_3$ phase shows that the dynamics of the quench has bypassed the formation of the intermediate $SmFe_3$ phase in favor of the nonequilibrium $SmFe_2$ phase.

The average grain size can be estimated from the X-ray diffraction line width using the Scherrer formula.[19] The value of 35 nm obtained by this technique is completely consistent with the grain size observed directly by electron microscopy, as noted above.

After nitriding for 4 h at 475 °C, the $Sm_2Fe_{17}$ X-ray diffraction lines shift to lower angles, as shown in Fig. 3(b), as nitrogen enters the lattice interstitially to form $Sm_2Fe_{17}N_x$. The characteristic diffraction pattern of the disordered $TbCu_7$ structure type is retained. The lattice expands from $a$ = 4.936 Å, $c$ = 4.147 Å for the unnitrided material to $a$ = 5.045 Å, $c$ = 4.218 Å for the nitrided powder, for a volume expansion of about 6.3%. The $SmFe_2$ peaks disappear, to be replaced by diffuse peaks corresponding to both αFe and SmN, indicating that some decomposition has occurred at the nitriding temperature. The line widths of the diffraction peaks are virtually unchanged, establishing that no significant grain growth has occurred during nitriding.

The nitriding temperature of 475 °C is close to the maximum temperature at which $Sm_2Fe_{17}N_x$ can be obtained successfully. Nitriding at a modestly higher temperature, such as 550 °C, promotes the decomposition of the $Sm_2Fe_{17}$ phase into SmN and αFe.

### 3.2 *Hysteresis Properties*

Coercivities of up to 15 kOe (1.2 MA/m) are generated in the $Sm_2Fe_{17}N_x$-based ribbons, as shown by the demagnetization curves in Fig. 4. The as-quenched ribbons (dashed curve) are magnetically soft, consistent with the low anisotropy of the disordered ($TbCu_7$-type) $Sm_2Fe_{17}$ phase. After nitriding for 4 h at 475 °C (solid curve), a coercivity of $H_{ci}$ = 15.3 kOe (1.22 MA/m) is obtained. There is a step in the demagnetization curve near zero field, which is attributable to the presence of magnetically soft αFe. The demagnetization curve exhibits a long tail extending into the third quadrant, characteristic of a material having a broad distribution of magnetization reversal fields. It is encouraging that no knee is observed in the curve even at the maximum applied field of −19 kOe (1.5 MA/m), implying that the highest values in the distribution of coercive fields are well in excess of this field.

The effect of $N_2$ exposure time at 480 °C on the coercivity $H_{ci}$ is shown by the open circles in Fig. 5. Maximum coercivity is achieved with nitriding times between 4 and 16 h.

## 4. Effect of Prenitriding Heat Treatment

The coercivity of Sm-Fe-N ribbon powders can be increased substantially by heat treating the powder prior to the nitriding step. Heat treatments were carried out at 700 °C for 1 h in an evacuated quartz tube. The sample was then furnace cooled to

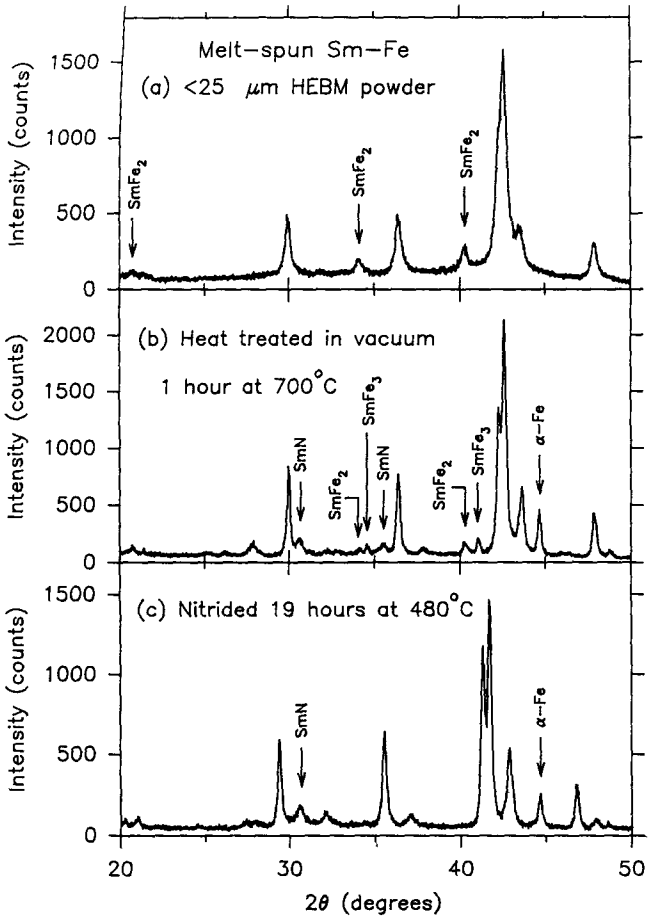


**Fig. 6** X-ray diffraction pattern for (a) high-energy ball milled powder, (b) HEBM powder after vacuum heat treatment for 1 h at 750 °C, and (c) the same powder after nitriding for 19 h at 480 °C.

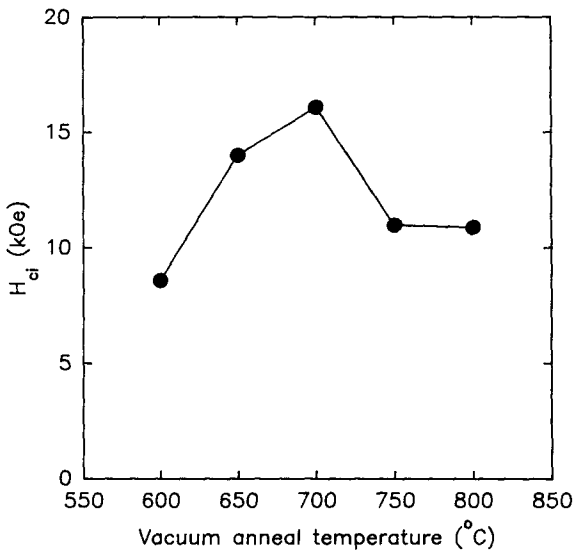


**Fig. 7** Coercivity $H_{ci}$ of nitrided ribbons as a function of the temperature used in the 1 h prenitriding vacuum heat treatment.

450 °C, and $N_2$ gas was introduced for times ranging from 1 to 64 h.

To be effective, the vacuum heat treatment requires a powder size of <25 μm (–500 mesh). Prenitriding heat treatment seemed to have little effect on the <45 μm (–325 mesh) powder, whose magnetics closely resemble that of Fig. 4. High-energy ball milling (HEBM) was selected as a convenient means for milling the ribbons to a –500 mesh powder. The ribbons were milled for 5 min in a SPEX 8000 mill, then sieved using a 500-mesh screen. Ball milling is used here only to reduce the ribbons to powder and is not intended to promote mechanical alloying. Unlike mechanical alloying, where long-time HEBM is used to produce an amorphous or finely microcrystalline alloy from elemental powders, there is no evidence that the authors' brief HEBM treatment materially alters the alloy microstructure already created by rapid quenching. The X-ray diffraction pattern of the <25μm powder, shown in Fig. 6(a), does not differ significantly from that of the as-quenched ribbons. When nitrided without vacuum heat treatment, the coercivity obtained is similar to that obtained with the larger <45μm powder.

The optimum vacuum treatment temperature was established by heat treating Sm-Fe ribbon powders at a range of temperatures between 600 and 800 °C for 1 h, followed by a standard nitriding procedure of 16 h at 450 °C in 140 kPa of $N_2$ gas. Figure 7 shows that the highest coercivity is obtained by heat treating at 700 °C.

Figure 6(b) shows the X-ray diffraction pattern after the 700 °C heat treatment. The disordered $TbCu_7$-type $Sm_2Fe_{17}$ pattern still predominates, although the line widths are somewhat narrower, indicating that modest grain growth has occurred. Close inspection reveals that some of the minor peaks characteristic of $Th_2Zn_{17}$-type $Sm_2Fe_{17}$, such as the 024 peak, are beginning to appear, but with only a fraction of their full intensity. Also, the $SmFe_2$ peaks are disappearing in favor of $SmFe_3$ peaks, as the alloy moves toward its equilibrium configuration. Finally, some αFe and SmN form during heat treatment. The latter is surprising, because $N_2$ has not yet been introduced and high-vacuum conditions were maintained throughout the anneal. One possibility is that some $N_2$ was carried into the system adsorbed on the powder and the quartz tube and was then effectively gettered by the Sm in the sample.

Upon nitriding, Fig. 6(c), the X-ray diffraction pattern closely resembles the pattern obtained without the vacuum heat treatment (Fig. 3), again except for hints of the $Th_2Zn_{17}$-type peaks beginning to emerge. The lattice constants are virtually identical ($a$ = 5.043 Å, $c$ = 4.218 Å, 6.2% volume expansion).

The effect of nitriding time at 450 °C on the coercivity is plotted as the solid circles in Fig. 5. Maximum coercivity is obtained by nitriding in the range of 450 to 480 °C for times ranging from 12 to 20 h. The demagnetization curve for the best sample, obtained by nitriding at 480 °C for 19 h following the 1 h 700 °C vacuum heat treatment, is shown in Fig. 8. Although the presence of αFe still produces a significant step in the demagnetization curve at low fields, limiting the remanence to 7.2 kG (0.72 T) and the energy product to 8.6 MGOe (68 kJ/m$^3$), the content of magnetically soft material is substantially reduced compared to the sample of Fig. 4, producing isotropic Sm-Fe-N ribbon powder with $H_{ci}$ = 22.3 kOe (1.77

MA/m). This value is similar to the coercivity typically produced in Nd-Fe-B melt-spun ribbons.

In conclusion, intrinsic coercivities of up to 22 kOe have been obtained by gas phase nitriding of melt-spun Sm-Fe ribbons. The hard magnetic properties are attributable to the favorable fine-grained microstructure generated by melt spinning, in concert with the excellent intrinsic magnetic properties generated by nitriding the $Sm_2Fe_{17}$ constituent phase to form $Sm_2Fe_{17}N_x$. The predominant form of $Sm_2Fe_{17}N_x$ in this high-coercivity material is the hexagonal $TbCu_7$-type structure, a disordered variant of the rhombohedral $Th_2Zn_{17}$ structure characteristic of equilibrium $Sm_2Fe_{17}$. The largest coercivity was obtained when Sm-Fe ribbon powder with a particle size <25 μm was first vacuum heat treated for 1 h at 700 °C, followed by gas phase nitriding for 19 h at 450 °C.

## Acknowledgments

The authors wish to thank Raja Mishra for supplying the transmission electron micrograph results for melt-spun Sm-Fe ribbons, as well as their colleagues Jan Herbst, Wes Capehart, and Greg Meisner for valuable discussions. Thanks go to Chuck Murphy and Dan Van Wingerden for preparing the Sm-Fe precursor ribbons. The authors are also grateful to Andy Wims, Jack Johnson, and Noel Potter of the Analytical Chemistry Department for the X-ray diffraction results and ICP composition analysis.

## References

1. J.J. Croat, J.F. Herbst, R.W. Lee, and F.E. Pinkerton, High-Energy Product Nd-Fe-B Permanent Magnets, *Appl. Phys. Lett.*, Vol 44 (No. 1), 1984, p 148-149
2. M. Sagawa, S. Fujimura, N. Togawa, H. Yamamoto, and Y. Matsuura, New Material for Permanent Magnets on a Base of Nd and Fe, *J. Appl. Phys.*, Vol 55 (No. 6), 1984, p 2083-2087
3. J.F. Herbst, J.J. Croat, F.E. Pinkerton, and W.B. Yelon, Relationships Between Crystal Structure and Magnetic Properties in $Nd_2Fe_{14}B$, *Phys. Rev B*, Vol 29 (No. 7), 1984, p 4176-4178
4. J.J. Croat, J.F. Herbst, R.W. Lee, and F.E. Pinkerton, Pr-Fe and Nd-Fe-Based Materials: A New Class of High-Performance Permanent Magnets, *J. Appl. Phys.*, Vol 55 (No. 6), 1984, p 2078-2082
5. F.E. Pinkerton and D.J. Van Wingerden, Magnetic Hardening of $SmFe_{10}V_2$ by Melt-Spinning, *IEEE Trans. Magn.*, Vol 25 (No. 5), 1989, p 3306-3308
6. J. Strzeszewski, Y.Z. Wang, E.W. Singleton, and G.C. Hadjipanayis, High Coercivity in $Sm(FeT)_{12}$ Type Magnets, *IEEE Trans. Magn.*, Vol 25(No. 5), 1989, p 3309-3311
7. M. Katter, J. Wecker, L. Schultz, and R. Grössinger, Preparation of Highly Coercive Sm-Fe-Ti by Rapid Quenching, *Appl. Phys. Lett.*, Vol 56 (No. 14), 1990, p 1377-1379
8. J.M.D. Coey and Hong Sun, Improved Magnetic Properties by Treatment of Iron-Based Rare Earth Intermetallic Compounds in Ammonia, *J. Magn. Magn. Mater.*, Vol 87 (No. 3), 1990, p L251-L254

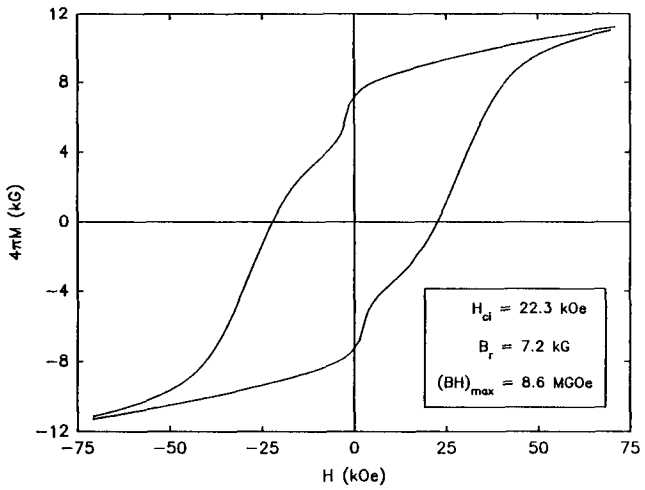


**Fig. 8** Demagnetization curve for high coercivity Sm-Fe-N ribbons.

9. Hong Sun, J.M.D. Coey, Y. Otani, and D.P.F. Hurley, Magnetic Properties of a New Series of Rare-Earth Iron Nitrides—$R_2Fe_{17}N_y$ ($y \sim 2.6$), *J. Phys. CM*, Vol 2 (No. 30), 1990, p 6465 ff
10. T.W. Capehart, R.K. Mishra, and F.E. Pinkerton, $Sm_2Fe_{17}N_x$: Site and Valence of the Interstitial Nitrogen, *Appl. Phys. Lett.*, Vol 58 (No.13), 1991, p 1395-1397
11. R.M. Ibberson, O. Moze, T.H. Jacobs, and K.H.J. Buschow, Nitrogen Atom Location in Rhombohedral and Hexagonal $Re_2Fe_{17}N_x$ Compounds, *J. Phys. Condens. Matter*, Vol 3 (No. 10), 1991, p 1219-1226
12. X.P. Zhong, R.J. Radwanski, F.R. de Boer, T.H. Jacobs, and K.H.J. Buschow, Magnetic and Crystallographic Characteristics of Rare-Earth Ternary Carbides Derived from $R_2Fe_{17}$ Compounds, *J. Magn. Magn. Mater.*, Vol 86 (No. 2-3), 1990, p 333-340
13. Ying-Chang Yang, Xiao-Dong Zhang, Lin-shu Kong, and Qi Pan, New Potential Hard Magnetic Material $NdTiFe_{11}N_x$, *Solid State Commun.*, Vol 78 (No. 4), 1991, p 317-320
14. M. Anagnostou, C. Christides, and D. Niarchos, Nitrogenation of the $RFe_{10}Mo_2$ ($R$ = Rare Earth) Compounds with $ThMn_{12}$ Type Structure, *Solid State Commun.*, Vol 78 (No. 8), 1991, p 681-684
15. F.E. Pinkerton and C.D. Fuerst, Magnetically Hard $Sm_2Fe_{17}N_x$ Prepared by Nitriding Melt-Spun Ribbons, *Appl. Phys. Lett.*, Vol 60 (No. 20), 1992, p 2558-2560
16. M. Katter, J. Wecker, and L. Schultz, Structural and Hard Magnetic Properties of Rapidly Solidified Sm-Fe-N, *J. Appl. Phys.*, Vol 70 (No. 6), 1991, p 3188-3196
17. R.K. Mishra, Microstructure of Melt-Spun Nd-Fe-B Magnequench Magnets, *J. Magn. Magn. Mater.*, Vol 54-57, 1986, p 450-456
18. Y. Khan, The Crystal Structures of $R_2Co_{17}$ Intermetallic Compounds, *Acta Crystallogr. B*, Vol 29, 1973, p 2502-2507
19. B.D. Cullity, *Elements of X-Ray Diffraction*, Addison-Wesley, 1956, p 97-99